

# Transfer bridge for Crushed Gypsum and Ash

**Nebojša Gnjatović**

Assistant Professor  
University of Belgrade  
Faculty of Mechanical Engineering

*Transfer bridges provide immense contribution to the efficient operation of high-capacity bulk material storages. The paper presents the design of one such system, used for transferring crushed gypsum and ash onto the barges docked in a storage facility, as well as the working technology, finite element strength and static stability analysis of the main substructures and the working devices. Due to the adjustments to the structure before its assembly, the analyses had to be repeated to account for the changes. Failureless operation of the presented transfer bridge represents an indirect validation of not only the presented results, but also the entire project, the stages of its development as well as the applied technology of manufacture and assembly.*

**Keywords:** transfer bridge, design, working technology, structure, strength.

## 1. INTRODUCTION

The transfer bridge TOR-1 (produced by "IVA Process Equipment" – Arandelovac, Serbia), Figure 1 and Table 1, is a part of the serially-coupled system of machines engaged in a facility which serves the purpose of storing and transferring the crushed gypsum and ash, created as a byproduct of desulfurization of the exhaust gases at the thermal power plant "Kostolac" in Serbia. The transport system within the facility consists of the analyzed transfer bridge TOR-1 and the stacker-reclaimer USKL [1,2], and is able to transport the material from the storage site, mix it with ash in the process and load it onto the docked barges which then transport it away from the facility. The method of operation of the gypsum and ash transferring facility is described in detail in [1].

Table 1. Basic technical data

Capacity	200 t/h
Span	10.5 m
Overhang	11.6 m
Total length	25.8 m
Total height	14.0 m
Track length	70.0 m



Figure 1. TOR-1 right after the assembly

## 2. MAIN SUBASSEMBLIES OF TOR-1

The main subassemblies of TOR-1 are:

- the load-bearing structure - gantry,
- the system of belt conveyors for the transport of gypsum,
- the chain conveyor for the transport of ash,
- the loading system consisting of two independent cascade loading device,
- the mechanism for the positioning of the transfer bridge,
- the subsystem for dedusting,
- the electrical equipment.

The load-bearing structure is of a gantry type, Figure 2, and made of the following segments: two frames (flexible (1) and rigid (2) leg), bearing platform (3), gantry (4) which is connected by a cylindrical joint to the bearing platform above the flexible leg, which connects the pairs of front (5) and rear (6) stays. The majority of the load-bearing structure is made of steel grade S235. The entire structure was assembled using welded and screw connections. The stays are connected to the load-bearing platform and the gantry via joints.

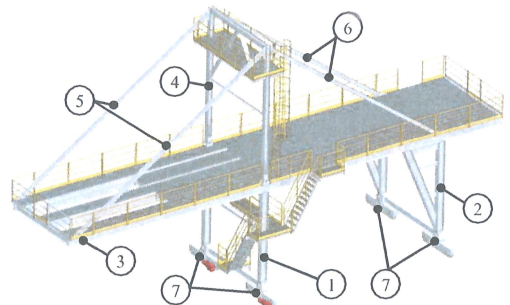


Figure 2. The load-bearing structure of the transfer bridge with the drive mechanism

The transfer bridge drive mechanism consists of 4 bogies (7), each with two wheels (400 mm in diameter), of which one is the driving wheel, Figure 2, and a 7.5 kW

Correspondence to: Nebojša Gnjatović, Assistant Professor  
Faculty of Mechanical Engineering,  
Kraljice Marije 16, 11120 Belgrade 35, Serbia  
E-mail: ngnjatovic@mas.bg.ac.rs

electric motor, for a total of  $4 \cdot 7.5 \text{ kW} = 30 \text{ kW}$ . Each of the bogie drives is frequency controlled, which allows for the efficient synchronisation during the positioning of the transfer bridge. The structure is supported on the two-wheel bogies via joints. The drive mechanism also includes the devices for the anchoring of the transfer bridge. The positioning of the of the transfer bridge is achieved via railway tracks with the axial distance of 10.5 m.

The system of belt conveyors consists of the fixed belt conveyor (TT1), with a variable inclination and the movable belt conveyor (TT2), and is used to load the crushed gypsu onto the barges. The movable belt conveyor is supported on the bearing platform via 4 wheels. Its own driving mechanism allows for two different positions, so that the barge can be loaded lengthwise from two spots, Figure 3.

Loading of the ash occurs via the chain conveyor (LT), which is fixed onto the bearing platform and has two discharge lids for the purpose of loading the barges, Figure 4.

The loading system consists of two independent discharge devices (KIU1 and KIU2), hanged on the lower girder of the bearing platform via hanging trolleys, Figures 3 and 4. The cascade discharge device is connected to the lower girder via two pairs of hanging self-driven trolleys, and consists of the transfer basket and the flexible loading nozzle which prevents the free falling of the material and ensures efficient dedusting. KIU1 follows the chain conveyor whereas KIU2 follows the belt conveyor (TT2). Each of the discharge spots in equipped with an efficient system for the prevention of dusting (DS), Figures 3 and 4.

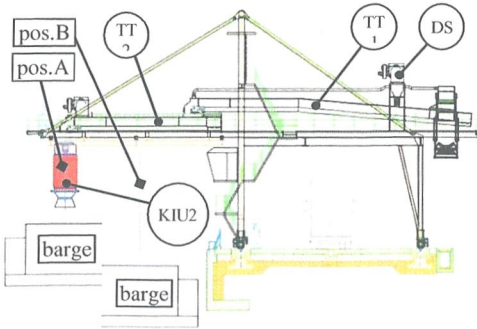


Figure 3. The system for the transport and loading of gypsum

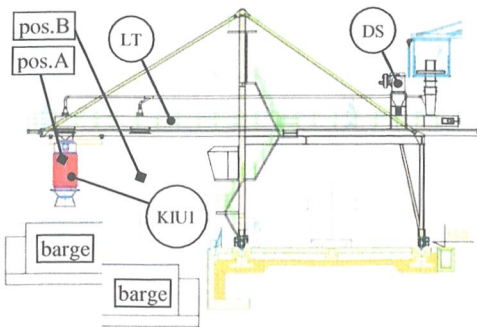


Figure 4 The system for transport and loading of ash

### 3. PRELIMINARY CALCULATIONS

The complexity and large mass of this machine demand a detailed analysis of stability and the position of the centre of gravity. Given the many possible configurations (combinations of positions of the working devices) during the loading process, it is necessary to define the load combinations (LCs) with an impact on the stability and the position of the center of gravity of the structure.

The load bearing structure of the transfer bridge is, apart from the deadweight, loaded by the weights of the fixed parts of the structure (service passageways, stairs, control cabine), weights of the working devices (belt conveyors, chain conveyor, loading devices) and the weight of the transported material on the working devices during the loading process.

The assessment of the working regime of the transfer bridge has yielded a conclusion that the gypsum loading and ash loading never occur simultaneously. Therefore, the first variable (*a*) in determining the LCs corresponding to the operation of the transfer bridge is:

- the transfer bridge is loading the ash, via the chain conveyor (LT) and
- the transfer bridge is loading the crushed gypsum, via the belt conveyors (TT1 and TT2).

The second variable (*b*) is devined by the position of the cascade discharge device (KIU). Each KIU can take one of two positions, Figures 3 and 4:

- KIU is in the position A, the position closer to the end of the overhang, and
- KIU is in the position B, the position closer to the flexible leg.

The third variable (*c*) corresponds to the condition of the cascade discharge device (KIU):

- KIU in the condition of nominal operation
- KIU in the condition of blockage.

A combination of the three variables yields a total of  $axbxc=16$  load combinations which can occur during the operation of the transfer bridge. Additionally, two specific load combinations were also considered, corresponding to the analysis of the effects of the hurricane wind on the structure (no transfer of material is occurring; both KIUs are either in the position A or the position B), Table 2.

Table 2. Load combinations

Device	Load combination (LC)																	
	Ash loading								Gypsum loading								None	
	1	2	3	4	5	6	7	8	9	10	11	12	13	14	15	16	17	18
LT	+	+	+	+	+	+	+	+	0	0	0	0	0	0	0	0	0	0
TT1	0	0	0	0	0	0	0	0	+	+	+	+	+	+	+	+	+	0
TT2	0	0	0	0	0	0	0	0	+	+	+	+	+	+	+	+	+	0
KIU1	N	Z	N	Z	N	Z	N	Z	N	N	N	N	N	N	N	N	N	N
pos.KIU 1	A	A	A	A	B	B	B	A	A	A	A	B	B	B	B	A	B	A
KIU2	N	N	N	N	N	N	N	N	Z	N	Z	N	Z	N	Z	N	Z	N
pos.KIU 2	A	B	B	A	A	B	B	A	B	A	B	A	B	A	B	A	B	A

A comprehensive analysis [3] has yielded a conclusion that in working conditions, both due to the weight of the analyzed structure and due to the most unfavorable position of its centre of gravity, the load combination LC2 is referent for the analysis of the stress-strain, static stability and the bearing capabilities of the driving mechanism of the transfer bridge. The action of



the hurricane wind on the structure out of operation has been analyzed for the LC17.

All of the presented analyses were conducted with the initial assumption that the bearing structure of the transfer bridge will be made of steel grade S355.

For the calculation of the structure under the basic loads (first load case – the action of wind is not taken into account), for which the safety factor of  $s_{I}=1.5$  was adopted, the load combination LC2\_1 (LC2 without the action of the wind in operation) was adopted as referent. In the second load case (safety factor  $s_{II}=1.33$ ), the load combination LC2\_2 (a lateral wind in operation is added to the load from the group LC2), was adopted as referent. The action of the lateral hurricane wind has been analyzed in the third load case (safety factor  $s_{III}=1.2$ ) for the load combination LC17 (which became LC17\_3).

Based on the data presented in Table 3, it can be concluded that the structure satisfies the strength criteria for all of the analyzed load cases.

**Table 3. The ratios between the permissible ( $\sigma_{per}$ ) and the maximum calculated ( $\sigma_{vM,max}$ ) stresses**

LC	$\sigma_{vM,max}$ (MPa)	Load Case	$\sigma_{per}$ (MPa)	$\sigma_{per}/\sigma_{vM,max}$
LC2_1	37.4	I	237	6.34
LC2_2	80.8	II	267	3.30
LC17_3	170.4	III	296	1.74

The maximum value of the calculated stress is obtained for the third load case, Table 3, and occurs in the zone of connection between the flexible leg and the bearing platform, Figure 5.

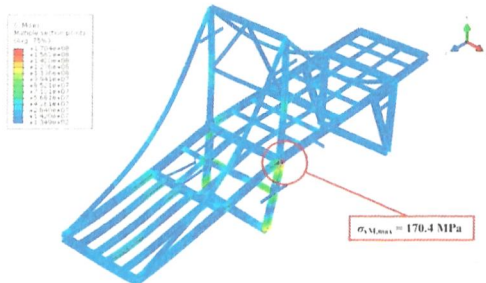


**Figure 5. The stress field for the load case LC17\_3**

The permissible deflections, shown in Table 4, have been determined using the following equations:

- the permissible deflection within the span -  $f_{1,per} = l_s/750 = 14.0$  mm,
  - the permissible deflection within the overhang -  $f_{2,per} = l_p/750 = 15.4$  mm,
  - the permissible deflection of the end of the overhang -  $f_{3,per} = l_p/300 = 38.6$  mm,
- where:  $l_s = 10500$  mm – the length of the span;  $l_p = 11587$  mm – the length of the overhang.

**Table 4. The ratios between the permissible ( $f_{per}$ ) and the maximum calculated ( $f_{max}$ ) deflections**

LC	$f_{max}$ (mm)			$f_{per}$ (mm)	$f_{per}/f_{max}$
	LC2_1	LC2_2	LC17_2		
span	1.57	1.98	2.62	14.0	5.34
overhang	9.95	9.58	9.75	15.4	1.55
overhang tip	7.42	7.42	6.53	38.6	5.20

Based on the data presented in Table 4, it can be concluded that the structure satisfies the criteria of permissible deformations under the effects of any of the analyzed LCs. The ratio between the permissible and the maximum calculated deflections has the lowest value in case which considers the deflection values within the span of the bearing platform under the effects of the load combination LC2\_1, Table 4 and Figure 6.

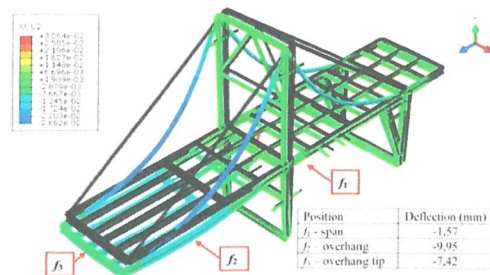


**Figure 6. The displacement field for the load case LC2\_1**

The maximum vertical load on the wheel occurs for the load combination LC17\_3 (the action of the hurricane wind on the structure out of operation), Table 5, and equals 170.8 kN, whereas the minimum vertical load on the wheel also occurs under the effects of the load combination LC17\_3 on the structure and equals 13.9 kN, leading to the conclusion that neither of the considered load combinations would jeopardize the static stability of the structure.

**Table 5. Vertical loads on the support wheels of the transfer bridge**

LC	Max. wheel load (kN)	Min. wheel load (kN)
LC2_1	132.6 kN	22.3 kN
LC2_2	150.6 kN	18.8 kN
LC17_3	170.8 kN	13.9 kN

#### 4. FINAL CALCULATIONS

During the production and assembly, the TOR structure, Figures 7 and 8, has undergone some adjustments:

- Due to unavailability of the material of desired quality (S355), the structure was made of steel grade S235 of significantly lower tensile properties
- In the zone at the end of the overhang of the bearing platform, positions of the main bearing elements were changed and additional bearing elements were added, in order to achieve adequate supporting of the conveyors and the bearing structure of the cover, Figure 7(b);
- For the purpose of easier transport and assembly, the connections between the elements of the bearing structure, screw connections were used, Figure 7(c);
- Due to technological reasons and meteorological conditions, a cover was installed on the structure in order to protect the mobile and fixed belt conveyors used to transport crushed gypsum and the chain conveyor used for the transport of ash, Figure 8;

- A counterweight was added to the right leg of the structure, significantly increasing the adhesive force acting on the drive wheels on the bogey of the rigid leg, Figure 8.

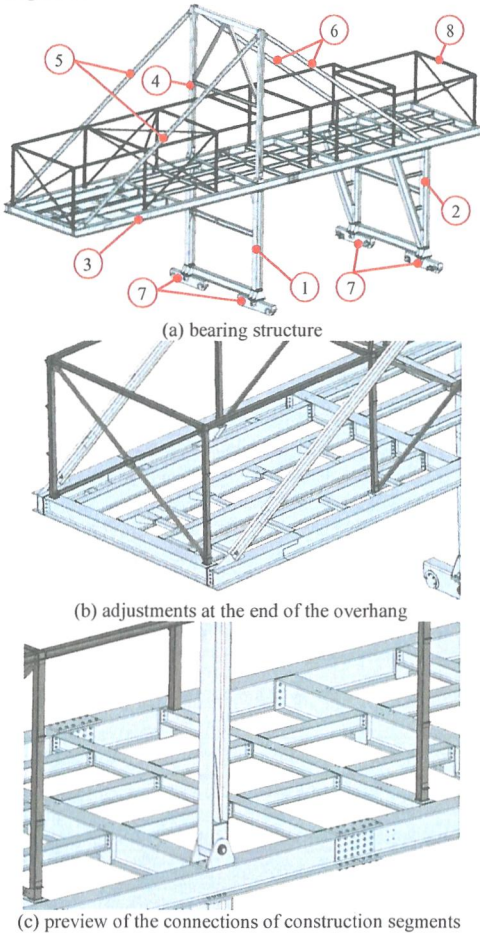


Figure 7. A 3D model of the bearing structure of the TOR-1 (1 – flexible leg; 2 – rigid leg; 3 – bearing platform; 4 – gantry; 5 – front stays; 6 – rear stays; 7 – bogeys; 8 – bearing structure for the cover)

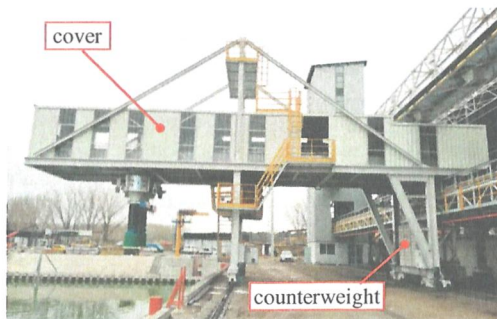


Figure 8. TOR-1 – final form

The installation of the cover had increased the mass of the structure by 6.62 t. Additionally, as a result, the gypsum and ash conveyors were completely covered. Consequently, in load combinations LC2\_2 and LC17\_3

(load combinations which account for the action of the lateral wind-in-operation and hurricane wind, defined as referent for the calculation of the stress-strain state of the structure in the preliminary calculations), the effects of the wind on said substructures were omitted. However, in considered load combinations, the action of the wind on the exposed frontal surface of the cover has been taken into account.

Given the fact that the structure operates in the outside environment, and considering the large area of the top side of the cover where snow can be piled up, the effects of the snow pile on the load bearing structure of the TOR was taken into account for the load combination LC2\_2 (for the snow pressure of  $q_s = 750 \text{ N/m}^2$  and the horizontal surface of the cover, the calculated mass of the snow is  $m_s = 8.53 \text{ t}$ ).

The addition of the counterweight had increased the total mass of the TOR structure by 10.27 t.

In total, the addition of the cover, the counterweight and the auxiliary connecting and supporting elements, the mass of the structure had changed from 58.14 t (which was the total mass of the base structure used in the preliminary analysis of the stress-strain state) to 75.80 t.

Taking into consideration all the changes to the design solution for the transfer bridge, in the continuation of the study, the impact of three referent load combinations, shown in Table 6, was analyzed.

Table 6. Referent load combinations

LC2	Deadweight	Material	Wind in operation	Hurricane wind	Snow
LC2_1	+	+	0	0	0
LC2_2	+	+	+	0	+
LC17_3	+	0	0	+	0

The stress fields in the referent zones of the structure, obtained for all of the analyzed load combinations are shown in Figures 9-11, while the maximum obtained values of calculated stress are provided in Table 7.

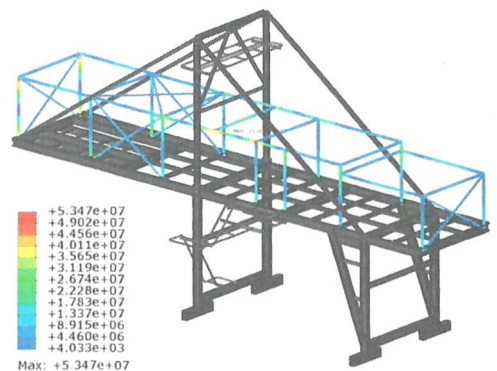


Figure 9. Stress field of the cover structure - LC2\_1

In the first and the second analyzed case (LC2\_1 and LC2\_2), the maximum stress values are obtained on the load bearing structure of the cover, Figures 9 and 10. These values are significantly lower than the permissible stress values for the considered load cases, Table 7.



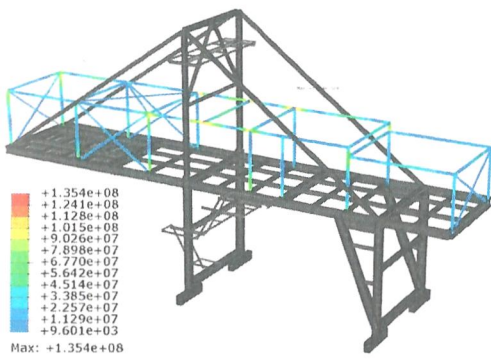


Figure 10. Stress field of the cover structure - LC2\_2

In the third case (LC17\_3), the maximum value of the stress occurs in the zone of connection between the flexible leg and the bogey, Figure 11. This value is very close to the permissible value for the third load case, also observed in the ratio between the maximum permissible and maximum calculated stress  $\sigma_{per}/\sigma_{vM,max} = 1.02$ , Table 7.

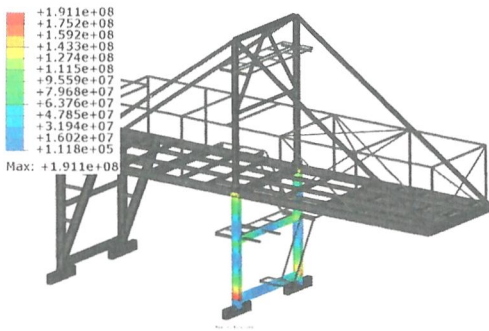


Figure 11. Stress field of the cover structure - LC2\_2

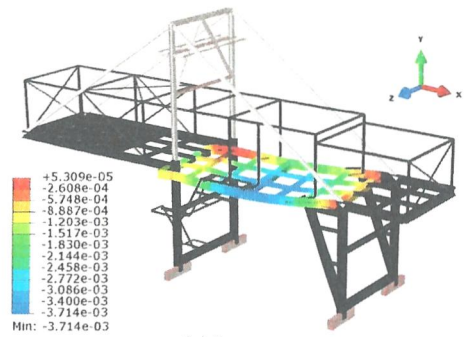
Table 7. The ratio between the permissible ( $\sigma_{per}$ ) and the maximum calculated ( $\sigma_{vM,max}$ ) stress values

LC	$\sigma_{vM,max}$ (MPa)	Load Case	$\sigma_{per}$ (MPa)	$\sigma_{per}/\sigma_{vM,max}$
LC2_1	53.5	I	157	3.12
LC2_2	135.4	II	177	1.30
LC17_3	191.1	III	196	1.02

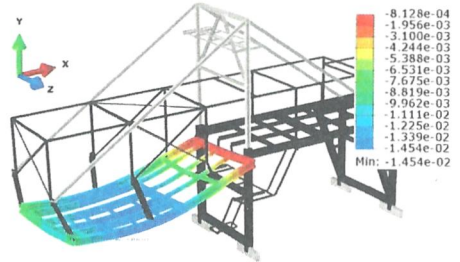
Figure 12 shows the displacement fields of the substructures of the bearing platform, refer for the proof of deformation for the load case LC2\_2. In all load cases, the maximum deflection values occur within the span of the bearing platform Table 8.

Table 8. The ratios between the permissible ( $f_{per}$ ) and the maximum calculated ( $f_{max}$ ) deflections

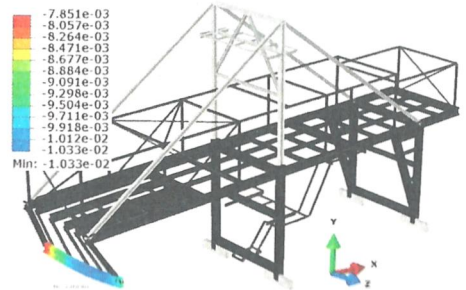
LC	$f_{max}$ (mm)			$f_{per}$ (mm)	$f_{per}/f_{max}$
	LC2_1	LC2_2	LC17_3		
span	2.9	3.7	4.3	14.0	3.26
overhang	12.1	14.5	11.9	15.4	1.06
overhang tip	9.1	10.3	8.6	38.6	3.72



(a) the span



(b) the overhang



(c) the end of the overhang

Figure 12. The displacement fields of the bearing structure - LC2\_2

Additional loads, corresponding to the extraordinary situations and not the nominal working loads, are considered in the proof of bearing capacity for the wheels via the factors which account for them:

- additional loads due to frontal wind-in-operation and the snow (maximum values) have the coefficient of factorization of the nominal bearing capacity of the wheels  $k_f^{II} = s_I/s_{II} = 1.5/1.33 = 1.13$ . Accordingly, the permissible loading of the wheel for the second load case is calculated according to the expression

$$P_{dop}^{II} = k_f^{II} \cdot P_{max} = 1.13 \cdot 185 = 209.0 \text{ kN},$$

- the extreme loading from the frontal hurricane wind (maximum values) has the coefficient of factorization of the nominal bearing capacity of the wheels  $k_f^{III} = s_I/s_{III} = 1.5/1.2 = 1.25$ . Accordingly, the permissible loading of the wheel for the third load case is calculated according to the expression

$$P_{dop}^{III} = k_f^{III} \cdot P_{max} = 1.25 \cdot 185 = 231.2 \text{ kN}.$$

The minimum vertical loading of the wheel occurs under the effects of the load combination LC17\_3 on the structure and equals 38.9 kN, Table 9. Therefore, it can be concluded that neither of the considered load combinations will jeopardize the static stability of the structure.

The calculated loads on the wheels, for all of the analyzed load combinations, satisfy the bearing criteria, Table 9.

**Table 9. The vertical loads on the wheels of the transfer bridge**

LC	Max. wheel load (kN)	Min. wheel load (kN)	Permissible wheel load (kN)
LC2_1	150.3	49.1	185.0
LC2_2	197.3	47.5	209.0
LC17_3	217.3	38.9	231.2

## 5. DISCUSSION AND CONCLUSION

The complexity of the analysis of behavior of the bearing structure of the transfer bridge is reflected, first and foremost, on the large number of possible relative positions of the working devices across the bearing platform. The capability of the structure to transfer two different types of material (gypsum and ash), which have to be transported via different types of transporters, adds an additional layer of complexity to both the design solution and the analysis of its behavior.

Significant changes to the design solution of the transfer bridge, resulting from the unavailability of the material of desired tensile properties (the structure was made out of steel grade S235 instead of the S355, planned in the preliminary calculations), but, mainly, technological reasons (which had imposed the installation of the cover over the belt and the chain conveyors) and the demand for the increased adhesive force on the rigid leg bogey wheels, have resulted in the increase of the total mass of the structure by 30.4%. Said adjustments have had a significant impact on the stress-strain state of the structure, as demonstrated by the following conclusions:

- although the structure, for all the analyzed load combinations in both the preliminary and the final calculations of the stress states, satisfies the strength criteria, the bearing reserve of the final design solution is considerably lower. Namely, the minimal ratio between the permissible and the maximum calculated stress was obtained for the load combination LC17\_3 and equals 1.74. Said value is 73.4% higher than the ratio obtained for the same load combination in the final calculations ( $\sigma_{per}/\sigma_{vM,max,LC17_3}=1.02$ );
- all the relevant segments of the bearing platform structure (the span, the overhang and the tip of the overhang) satisfy the criteria of permissible displacements, in both the preliminary and the final calculations for all of the analyzed load combinations;
- the minimal ratio between the permissible and the maximum calculated deflection, in the preliminary calculations, was obtained for the load combination LC2\_1 and equals  $f_{per}/f_{max,LC2_1}=1.55$ . Said value is considerably higher than the minimal value of the respective ratio obtained in the final calculations, which

was obtained for the load combination LC2\_2 and equals  $f_{per}/f_{max,LC2_2}=1.06$ ;

- installation of the 10.27 t counterweight has resulted in a significant increase of the adhesive force on the bogey wheels of the rigid leg, a claim supported by the fact that the minimum wheel force has increased from 13.9 kN (LC17\_3, preliminary calculations) to 38.9 kN (LC17\_3 – final calculations). Therefore, the minimal wheel force is 2.8 times higher at the assembled structure;
- neither of the considered calculation case will result in jeopardized static stability of the structure;
- calculated loads of the wheels, for all of the analyzed load combinations, in both the preliminary and the final calculations, satisfy the bearing criteria.

Finally, a two-year failureless exploitation of the analyzed transfer bridge TOR-1 acts as an indirect validation of not only the presented results, but the entire design project, the stages of its development and the technology of manufacture and assembly.

## ACKNOWLEDGMENT

This work is a contribution to the Ministry of Education, Science and Technological Development of Serbia funded project "Integrated research in the fields of macro, micro and nano mechanical engineering" (Contract number: 451-03-68/2022-14/200105).

## REFERENCES

- [1] N. Gnjatović, S. Bošnjak, I. Milenović, A. Stefanović, M. Urošević, *Gantry Bucket Chain Stacker-Reclaimer for Crushed Gypsum*, in: S. Bošnjak, N. Zrnić & G. Kartnig (Eds.), *Proceedings of the 24<sup>th</sup> International conference on Material handling, constructions and logistics (MHCL '22)*, Belgrade (Serbia), 2022, University of Belgrade - Faculty of Mechanical Engineering, Belgrade, 2022, pp. 47–54.
- [2] Bošnjak, S., Gnjatović, N., Milenović, I., Stefanović, A., Urošević, M.: *Strength calculation of the stacker-reclaimer "USKL" structure (in Serbian)*, realized for "IVA Process Equipment" - Arandjelovac (Serbia), University of Belgrade-Faculty of Mechanical Engineering, Belgrade, 2019.
- [3] Bošnjak, S., Gnjatović, N., Milenović, I.: *Preliminary strength calculation of the transfer bridge "TOR-1" structure (in Serbian)*, realized for "IVA Process Equipment" - Arandjelovac (Serbia), University of Belgrade-Faculty of Mechanical Engineering, Belgrade, 2017.
- [4] Bošnjak, S., Gnjatović, N., Milenović, I., Stefanović, A., Urošević, M.: *Strength calculation of the transfer bridge "TOR-1" (in Serbian)*, realized for "IVA Process Equipment" - Arandjelovac (Serbia), University of Belgrade-Faculty of Mechanical Engineering, Belgrade, 2018.